*Proceedings of the 6th International Conference on Gas Hydrates (ICGH 2008), Vancouver, British Columbia, CANADA, July 6-10, 2008*

# PETROLEUM HYDRATE DEPOSITION MECHANISMS: THE INFLUENCE OF PIPELINE WETTABILITY

**Guro Aspenes [*,1,2], Sylvi Høiland [2], Tanja Barth [1], Kjell Magne Askvik [3], Ramesh A. Kini [4] and Roar Larsen [2]**

[1] **University of Bergen, Department of Chemistry, Bergen, Norway**
[2] **SINTEF Petroleum Research, Norway**
[3] **StatoilHydro R&D, Bergen, Norway**
[4] **Chevron Energy Technology Company, Houston, TX, USA**

## ABSTRACT

The mechanisms by which hydrates deposit in a petroleum production-line are likely to be related to pipeline surface properties, e.g. pipeline material, surface energy and roughness. In this work, the wettability alteration of pipeline surfaces from contact with oil, as well as the adhesion energy between water and solid in the presence of oil is investigated. Contact angles are determined as a function of solid material and oil composition, for both model oils and crude oils. Although contact angles in oil/brine/solid systems have been extensively reported in the literature, the variety of solids that may mimic a pipeline is limited. In this study, we include various metal surfaces in addition to glass and a coating. Initial results from using near infrared imaging for collecting contact angle data in non-translucent systems are also presented.

*Keywords:* deposition, adhesion, pipeline, metal surface, wettability, surface energy, hydrate

## NOMENCLATURE

$W_{abc}$ Adhesion energy in a three phase system
$\theta$ Contact angle
$\gamma_{ab}$ Interfacial tension between phase a and b

## INTRODUCTION

Pipelines used for petroleum transportation are affected over time by the fluids and solids which are contacting them, giving rise to e.g. corrosion, coating by an oil or wax/asphaltene layer or/and general wear of the pipeline. The deposition of hydrates in a production line is likely to be affected by the state of the pipe wall. The molecular forces governing the attraction between two solids, e.g. two hydrate particles or hydrate particle and pipe wall, in the presence of oil and/or water, may be quantified through the adhesion energy. The adhesion energy depends on the interfacial tensions between the involved phases. For solid surfaces in contact with crude oil and water, the interfacial tensions, and hence the wettability of the system, are influenced by adsorption of crude oil components [1], giving wettability states ranging from water- to oil-wet. The formation of oil-wet hydrates correlates with non-agglomerating behavior and low hydrate plugging tendency [2].

For hydrates that form and grow from a water droplet stuck on the pipe wall, as well as for flowing hydrate particles adhering to the wall, the adhesion energy depends on pipeline wettability. For instance, a water drop is more likely to adhere to a water-wet than an oil-wet pipe wall. Particle-particle adhesion has been studied to some extent [3], while the effect of wettability of the pipeline wall is, to the best of our knowledge, not studied in the same degree.

In the present work, the effect of crude oil on pipeline wettability has been studied. As long as the adhesion between hydrate particles and between

[*]Corresponding author: Phone:+47 55 54 39 08 Fax: +47 55 54 39 05 Email: guro.aspenes@iku.sintef.no

hydrate particles and the wall are low, hydrate deposition and plugging are presumably minor problems, unless particle loadings are high. A goal is to make the hydrates flow with the stream as a dispersion. It has been shown that acid fractions from a non-plugging oil can be added to a plugging oil to change its hydrate plugging tendency into non-plugging [2, 4]. Some biosurfactants have shown to have the same effect [4, 5].

The wettability of a solid can be quantified by the angle $\theta$ in the three-phase contact point of a liquid drop in thermal equilibrium on a horizontal surface. The contact angle $\theta$ is defined here as the angle measured through the aqueous phase, see Figure 1.

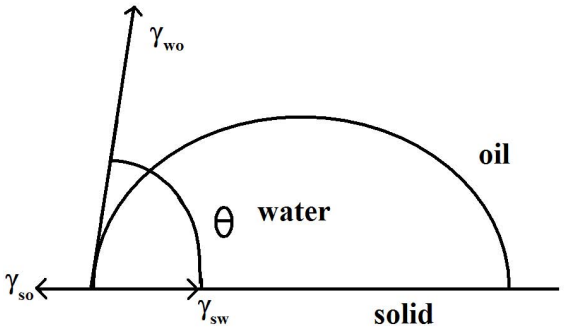


Figure 1: Sketch of a sessile drop, oil/water/solid system.

The relationship between interfacial tension and contact angle was established by Young [6] and is generally known as Young's equation

$$cos\theta = \frac{\gamma_{so} - \gamma_{sw}}{\gamma_{wo}} \quad (1)$$

where $\gamma$ is the interfacial tensions between the three different interfaces solid/oil, solid/water and water/oil. Surfaces with contact angles lower than 90 degrees are considered as water-wet, whereas angles larger than 120 degrees correspond to oil-wet surfaces. For the intermediate angles, the surfaces have no preference for one or the other liquid phases.

## MATERIALS AND METHODS

## Materials

The solid surfaces that have been investigated are stainless steel (AISI 316 L), aluminum (EN AW 5052), brass (63% Cu, 37% Zn), glass, quartz and two epoxy surfaces coated in two different ways (Epoxy-A and Epoxy B). The surfaces have been washed thoroughly with a detergent (sodosil (RM 01) from Riedel-de Haën) and soaked in distilled water. The surfaces were then flushed with ethanol (p.a. quality) before drying the surface with nitrogen gas directly before use.

The model oil consists of petroleum ether (J. T. Baker and Riedel-de Haën, boiling range 60-80 °C) with commercial naphthenic acids (Aldrich) in concentrations ranging from 0 to 5000 ppm.

The aqueous phase is a buffer solution (titrisol from Merck) of pH 6 ($\pm$ 0.05), consisting of 0.16 mol/l NaOH (aq) and 0.06 mol/l citric acid (aq) ($C_6H_8O_7$).

The crude oil is supplied by StatoilHydro ASA and given the name B4c.

### *Metal surfaces*

The composition of the different metal alloys was given by the supplier, and has been verified through x-ray element analysis. All the metal surfaces are covered with an oxide layer [7].

The stainless steel alloy consists of approximately 18 % chromium, 12 % nickel, 2 % molybdenium, small traces of carbon and silicon and approximately 68 % iron. The surface composition of the stainless steel surface is dependent on chemical composition, temperature and pH of the aqueous solution with which the solid metal is in contact. At low pH (<6) and in air at room temperature a spontaneous formation of a protective surface layer makes the stainless steel corrosion resistant. The main components of the passive layer are insoluble chromium ($Cr_2O_3$ and/or $Cr(OH)_3$) and traces of iron oxide (mostly $Fe_2O_3$) [8–10].

The aluminum alloy has approximately 2 % magnesium and traces of silicon, iron, copper, manganese and zinc with amounts varying from 0.1 to 0.5 %, giving an amount of aluminum of approximately 96 %. Due to the high reactivity of aluminum, with reduction potential of -1.66 volts, the surface consists of a thin layer of $Al_2O_3$ which protects the surface from further reaction and is rapidly self-healing when scratched.

Both alloying elements of the brass alloy react with oxygen in air giving copper oxide (CuO) and zinc oxide (ZnO).

### *Glass surfaces*

The quartz cells mainly consist of silicon oxide ($SiO_2$), while optical glass is silicon oxide containing some impurities such as borate. For the model oil systems glass cells were used, while both quartz and glass were used in the crude oil experiments.

### *Epoxy coated surfaces*

The epoxy coating delivered from Jotun AS consists of two parts that is mixed shortly before use. Part A consists of bis(oxyranylmethyl)ether Bisphenol F (50-100 %), alcyl (c10-c16) glycidyl ether (2,5-10 %) and benzyl alcohol (2,5-10 %). Part B consists of 3,6-diazaoctanethylenediamin (10-25 %). The final composition consists of 6.5 parts of A and 1 part of B by volume. Jotun AS state that the coating has excellent durability against solvents and chemicals and very good durability against water.

The surfaces were rinsed before coating. The coating was applied to all the different metals (Aluminum, Brass and Steel). However, the type of metal used showed to have no effect on the measured contact angles on the surfaces, since the layer of epoxy was fairly thick. When the two parts A and B were mixed the blend behaved like glue, making it difficult to obtain an even and smooth layer. Two methods were used to coat the metal surfaces, named epoxy-A and epoxy-B. Epoxy-A was obtained by simply applying the coating to the surfaces and polish it with sand paper (P80) after hardening, giving a rather smooth surface. Epoxy-B was obtained by diluting the mixed coating in acetone (proportion $\sim$ 1 g epoxy : 1 ml acetone) and pouring the solution over the surfaces. Epoxy-B was a bit rougher than Epoxy-A from a visual point of view.

## Methods

### *Contact angle measurements*

All experiments were performed at room temperature, approximately 21 °C. The metal surfaces were aged in the oil solution for approximately 24 hours. For the model oil systems the surfaces were submerged in a glass cell which was filled with petroleum ether containing naphthenic acid with concentrations ranging from 0 to 5000 ppm. A water drop (buffer) was deposited on the surface.

For the experiments with crude oils the cuvettes (quartz and glass, 1x1 cm) were aged in the oil for approximately 24 hours at approximately 50 °C to avoid wax precipitation. The same brine used for the model oil systems (buffer solution, pH 6) was employed.

The contact angles were determined from image analysis. The camera used is a Retiga Exi fast 1394 from QIMAGING with a spectral response between 400 and 1000 nm. This camera is connected to a microscope (SMZ800) from Nikon. The software used is ImagePro Plus.

Near Infrared imaging has been used for collecting contact angle data in non-transparent systems. An optical filter delivered from Edmund Optics with reflection below 800 nm (RM-90) was used to take advantage of the most transparent region of the oil. The light source used is a Quartz Tungsten Halogen lamp delivered from Newport, with a maximum spectral efficiency between 500 and 1500 nm.

All angles have been evaluated using an axisymmetric drop shape analysis - profile (ADSA-P) method that measures the angle from the complete drop shape profile. The contact angle can also be determined by manually setting the tangent, but this method is associated with some degree of subjectivity [11]. The ADSA-P determines the contact angle from combining interfacial tension and gravity properties.

Between 8 and 12 parallel measurements were performed for each system, and the standard deviation calculated.

### *Interfacial tension*

The interfacial tensions, $\gamma$, were measured by the drop weight method [12], using Harkins-Brown equation [13]

$$\gamma = \frac{(V\Delta\rho g)}{(2\pi r F)} \tag{2}$$

where V is the drop volume, $\Delta\rho$, is the difference in density of the two phases, g is the acceleration due to gravity (g = 9,81 m/s$^2$), r is the radius of the needle, and F is a correction factor which is based on the radius of the needle and the volume of the droplet. The densities were determined using an Anton Paar DMS60 densitometer connected to an Anton Paar DMA602HT measuring cell.

### *Surface energy*

The state of a solid surface can be quantified through its surface energy. By approximation, this can be determined by using the "equation of state for interfacial tension" (EOS) [14]:

$$\gamma_{sl} = \gamma_{lv} + \gamma_{sv} - 2\sqrt{\gamma_{lv}\gamma_{sv}}e^{-\beta(\gamma_{lv}-\gamma_{sv})^2} \quad (3)$$

$\beta$ is a constant that has been determined empirically and has an average value of 0.0001247 $(\text{mJ/m}^2)^{-2}$ [15]. This equation is used for measurements in solid, liquid, vapour (slv) systems, hence the denotions. If the equation above is combined with the Young equation (1), the following relation is obtained:

$$cos\theta = -1 + 2\sqrt{\frac{\gamma_{sv}}{\gamma_{lv}}}e^{-\beta(\gamma_{lv}-\gamma_{sv})^2} \quad (4)$$

The solid surface energy, $\gamma_{sv}$, can be determined from this equation using various probe fluids with different surface tensions resulting in different contact angles, $\theta$. This determination comprises some basic assumptions such as no interaction between the air and solid surface and that the air can be equalized with vacuum. The determination also assumes that there is no chemical reaction between solid and probe fluid.

One challenge related to this procedure is that the fluid surface tension, $\gamma_{lv}$, must be larger than the surface energy, $\gamma_{sv}$ [15]. This can be explained by the spreading coefficient $S_{ls}$, given by the equation [16]:

$$S_{ls} = \gamma_{sv} - \gamma_{lv} - \gamma_{sl} \quad (5)$$

If $S_{ls} > 0$ the liquid will spread on the solid surface. Most of the fluids that were tested in this work spread on the surfaces. The choice of fluids not spreading was limited to DMSO, formamide, glycerol and water. This indicates that the surfaces in this work are highly energetic, as should be expected.

In literature, almost no measurements of surface energies of metals are reported from using this method. Most of the available experimental surface energy data of metals are obtained from surface tension measurements in the liquid state and extrapolated to zero temperature [17]. These values are in the order of 1000 to 2000 $\text{mJ/m}^2$ at approximately 300 Kelvin. This gives quite different values than from determining surface energy from solid state with contact angle measurements.

### *Adhesion energy*

The contact angle can be used to determine the adhesion energy, which is calculated from rewriting Young's equation into the Young-Dupré equation [18]:

$$W_{swo} = \gamma_{wo}(1 + cos\theta) \quad (6)$$

The adhesion energy, $W_{swo}$, gives the adhesion energy per unit area of a solid surface (s) and water (w) adhering in oil (o), and thus comprises both interfacial tension, $\gamma_{wo}$, between the brine and oil phase, and contact angle, $\theta$, into one parameter.

## RESULTS AND DISCUSSION

### *Surface energy*

As mentioned, surface energy showed to be difficult to measure for such highly energetic surfaces as metal surfaces and glass, due to spreading conditions for most of the probe fluids. Fluids such as hexane, heptane, decane and benzene with surface tensions between 18 and 28 $\text{mJ/m}^2$ spread on all the surfaces while the fluids with higher surface tension than 45 $\text{mJ/m}^2$ could be used on some of the surfaces. An example of surface energy determination (brass) is shown in Table 1.

Table 1: Surface energy determined for brass.

| Probe fluids | Surface tension $\gamma(\text{mJ/m}^2)$ | Angle $\theta$(degrees) | Surface energy $\gamma(\text{mJ/m}^2)$ |
|---|---|---|---|
| Hexane | 18.5* | Spreading | - |
| Heptane | 20.3* | Spreading | - |
| Decane | 23.9* | Spreading | - |
| Benzene | 28.9* | Spreading | - |
| DMSO | 45.1 | $20.6 \pm 2$ | 42.3 |
| Formamide | 59.2 | $45.8 \pm 2$ | 42.9 |
| Glycerol | 65.7 | $47.5 \pm 2$ | 46.4 |
| Water(dist) | 73.0 | $53.2 \pm 3$ | 46.9 |
| Water(buffer) | 73.6 | $55.4 \pm 3$ | 45.6 |
| Average | | | $45 \pm 2$ |

*Values from literature [15].

The "equation of state for interfacial tension" (EOS) method, see Equation 4, was used for determining the surface energy for all the surfaces , i.e. stainless steel, glass, aluminum and epoxy coated surfaces. The average values and standard deviations from these experiments are given in Table 2 and Figure 2. The variation between some of the values obtained was rather large and obvious outliers were eliminated from the data set.

Table 2: Surface energies for all the solids.

| Solid surface | Surface energy $\gamma$(mJ/m$^2$) | Probe fluids used |
|---|---|---|
| Epoxy-A | $24 \pm 2$ | 3 |
| Epoxy-B | $29 \pm 2$ | 4 |
| Brass | $45 \pm 2$ | 5 |
| Aluminum | $59 \pm 1$ | 2 |
| Stainless steel | $64 \pm 5$ | 2 |
| Glass | 65 | 1 |

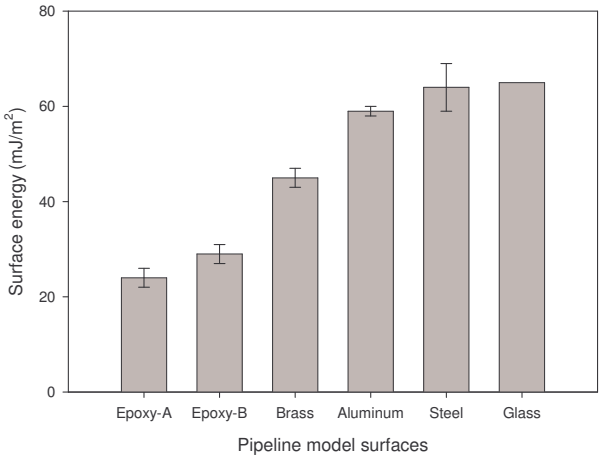


Figure 2: The different surface energies studied in this work.

Podgornik et al. [19] recently reported surface energy for steel determined with contact angle measurements and probe fluids, giving a value of approximately 30 mJ/m$^2$. This is somewhat lower than the value determined in this work, but it should be noted that our material is stainless steel.
The surface energies for the solids range from 24 to 65 mJ/m$^2$. For glass, only one probe fluid could be used. Therefore, the value given for glass has no standard deviation.

### *Model oils*

As mentioned above, it has been shown that acid fractions can change the hydrate plugging tendency by making the hydrate surface less water-wet [4].
A wettability alteration of the pipeline towards less water-wet behavior from adsorption of e.g. petroleum acids, is likely to reduce the possibility of hydrate deposition, and thus the plugging tendency.
The results from the contact angle measurements are presented in Table 3 and Figures 3 and 4. The figures show the contact angles as a function of acid concentration. The results are presented in two separate graphs, Figure 3 and 4, because the acids seem to have different adsorption behavior on the different surfaces. Figure 3 illustrates the metal surfaces, while Figure 4 illustrates the glass and epoxy coated surfaces.

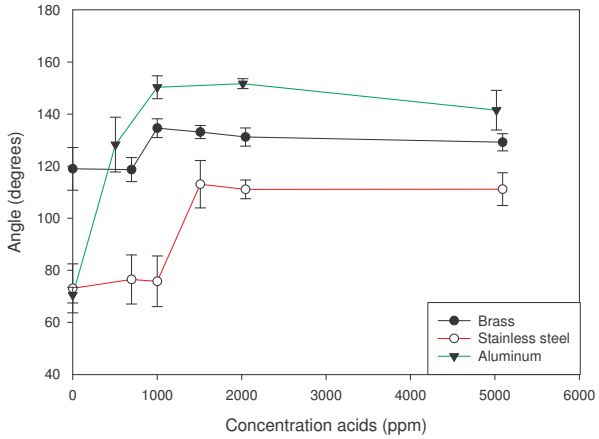


Figure 3: Contact angles of water drops on metal surfaces in petroleum ether with different concentration of naphthenic acids.

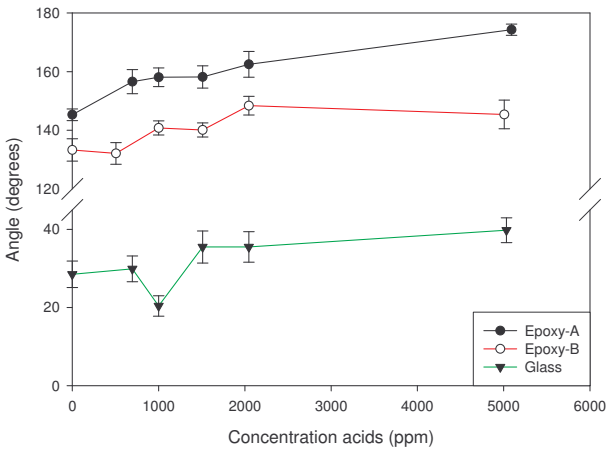


Figure 4: Contact angles of water drops on glass and coated surfaces in petroleum ether with different concentration of naphthenic acids.

From the graphs we can see that the angles increase with increasing concentration of acids, i.e. towards more oil-wet conditions. Thus, the experiments in this work show that petroleum acids are able to change the wettability of the pipe surface, in a similar manner as it can change the wettability of the

Table 3: Measured angles of buffer drops on different surfaces with different concentrations of naphthenic acids in petroleum ether.

| Concentration Naphthenic acids ppm | Epoxy-A Angle $\theta$ $(degrees)$ | Epoxy-B Angle $\theta$ $(degrees)$ | Brass Angle $\theta$ $(degrees)$ | Aluminum Angle $\theta$ $(degrees)$ | Steel Angle $\theta$ $(degrees)$ | Glass Angle $\theta$ $(degrees)$ |
|---|---|---|---|---|---|---|
| 0 | $145 \pm 2$ | $133 \pm 4$ | $119 \pm 8$ | $71 \pm 3$ | $73 \pm 9$ | $29 \pm 3$ |
| 500 | - | $132 \pm 4$ | - | $128 \pm 11$ | - | - |
| 700 | $157 \pm 4$ | - | $119 \pm 5$ | - | $77 \pm 9$ | $30 \pm 3$ |
| 1000 | $158 \pm 3$ | $141 \pm 2$ | $135 \pm 4$ | $150 \pm 4$ | $76 \pm 10$ | $20 \pm 3$ |
| 1500 | $158 \pm 4$ | $140 \pm 2$ | $133 \pm 3$ | - | $113 \pm 9$ | $36 \pm 4$ |
| 2000 | $163 \pm 4$ | $148 \pm 3$ | $131 \pm 4$ | $152 \pm 2$ | $111 \pm 4$ | $36 \pm 4$ |
| 5000 | $174 \pm 2$ | $145 \pm 5$ | $129 \pm 3$ | $142 \pm 8$ | $111 \pm 6$ | $40 \pm 3$ |

hydrate surface.

The change in wettability is likely to be caused by adsorption of acids onto the surfaces. The surfaces seem to get saturated with acid molecules at different concentrations. The metal surfaces have saturation limits at approximately 1000-1500 ppm of acids, while the other surfaces have a rather smooth increase from 0 to 5000 ppm of acids. The aluminum surface is most influenced by the acids, while brass is the least affected surface as far as the metal surfaces are concerned. The standard deviations of the measurements are rather large, which is true for most contact angle measurements, in general [15].

The two different epoxy coated surfaces give different contact angles even though they are made of the same material. The two curves are virtually the same but only with an upward shift. The difference can be due to different physical structure of the coating, such as surface roughness.

The interfacial tension between petroleum ether, with different concentrations of naphthenic acids, and buffer solution is shown in Figure 5. This can be combined with the contact angles to give an adhesion energy, as defined in Equation 6. The value obtained indicates the adhesion energy between brine (buffer) and a solid surface in the presence of oil. The adhesion energies are given in Table 4.

Adhesion energy as a function of acid concentration is shown in Figures 6 and 7.

Figure 6 illustrates the metal surfaces, while Figure 7 illustrates the glass and epoxy coated surfaces. The curves are similar to the results from the contact angle measurements, only inverted. The results indicate that the adhesion of water to a solid surface decrease with increasing concentrations of acids in

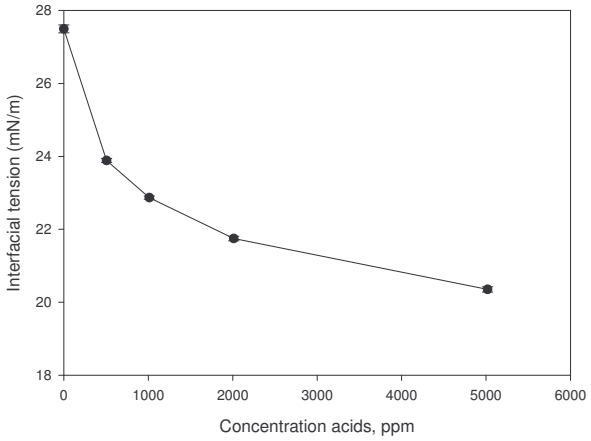


Figure 5: Interfacial tension between buffer solution and petroleum ether with different concentrations of naphthenic acids.

an oil/brine/solid system.

In order to fully understand what actually happens for each of the surfaces the surface-acid interactions are important. This is beyond the scope of this present paper. However, some brief considerations are given below.

The interaction is believed to be driven by a Lewis Brønsted type acid-base chemisorption between the reactive carboxylic acid head and specific surface reactive sites on the metal surfaces [20–23].

Different chemical reactions results in different orientation of acids on the surfaces [23]. The different effect of acids on the contact angles on metal surfaces has been suggested to occur due to difference in reactivity [24], where aluminum is a more reactive metal than the other metal samples tested here.

There seems to be a correlation between adhesion

Table 4: Adhesion energy between buffer solution and different surfaces, in different concentrations of naphthenic acids in petroleum ether.

| Concentration Naphthenic acids ppm | Epoxy-A Adhesion energy $mJ/m^2$ | Epoxy-B Adhesion energy $mJ/m^2$ | Brass Adhesion energy $mJ/m^2$ | Aluminum Adhesion energy $mJ/m^2$ | Steel Adhesion energy $mJ/m^2$ | Glass Adhesion energy $mJ/m^2$ |
|---|---|---|---|---|---|---|
| 0 | $5 \pm 1$ | $9 \pm 1$ | $14 \pm 3$ | $36 \pm 1$ | $36 \pm 4$ | $52 \pm 1$ |
| 500 | - | $8 \pm 1$ | - | $9 \pm 4$ | - | - |
| 700 | $2 \pm 1$ | - | $12 \pm 2$ | - | $29 \pm 4$ | $44 \pm 1$ |
| 1000 | $2 \pm 0$ | $5 \pm 1$ | $7 \pm 1$ | $3 \pm 1$ | $28 \pm 4$ | $44 \pm 0$ |
| 1500 | $2 \pm 1$ | $5 \pm 1$ | $7 \pm 1$ | - | $14 \pm 3$ | $40 \pm 1$ |
| 2000 | $1 \pm 0$ | $3 \pm 1$ | $7 \pm 1$ | $3 \pm 0$ | $14 \pm 1$ | $39 \pm 1$ |
| 5000 | $0 \pm 0$ | $4 \pm 1$ | $8 \pm 1$ | $4 \pm 2$ | $13 \pm 2$ | $36 \pm 1$ |

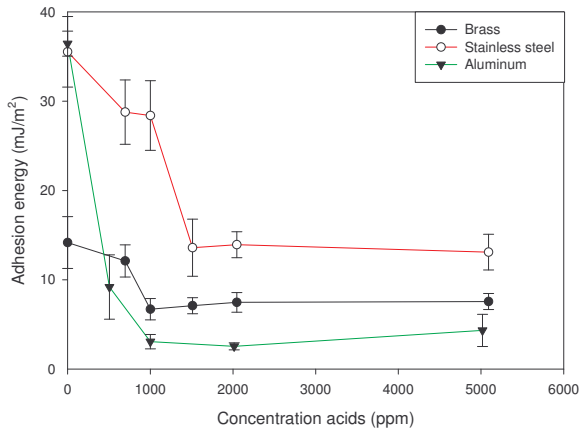


Figure 6: Adhesion energy between buffer solution and metal surfaces in petroleum ether with different concentrations of naphthenic acids.

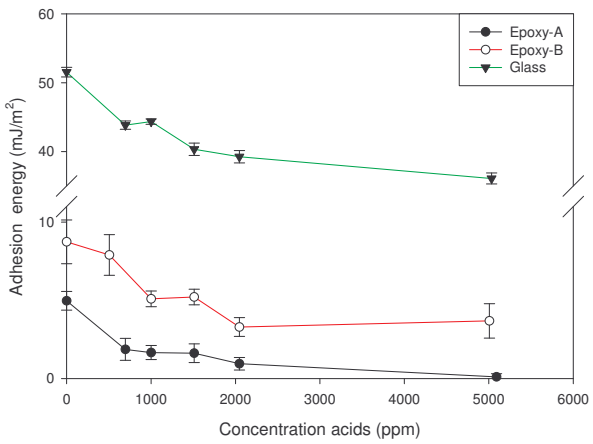


Figure 7: Adhesion energy between buffer solution and glass and coated surfaces in petroleum ether with different concentrations of naphthenic acids.

energy and solid surface energy. This is shown in Figure 8. The adhesion of water to a solid surface in oil is lower on surfaces with low surface energies, meaning that the aqueous phase has less tendency to stick to these surfaces. The graph also shows the decrease in adhesion energy as the concentration of acids is increased. The surfaces have become more oil-wet.

Aluminum deviates somewhat from the other surfaces, most likely because of surface reaction with the acids.

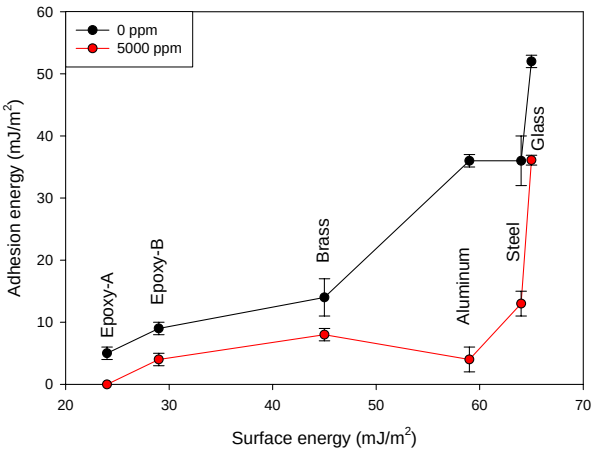


Figure 8: Correlation between solid surface energy and adhesion energy of brine in petroleum ether with different concentrations of acids, 0 and 5000 ppm.

The relevance of this fundamental work to realistic pipeline surfaces, being rough and corroded, might be discussed, but the surfaces employed in this work are nevertheless representative for materials frequently used in laboratory equipment. Hence,

the results are of direct value for understanding the influence of pipeline wettability on hydrate deposition in e.g. wheel tests and bench scale flow loops. From experimental observations during wheel tests, a water drop stuck on the pipe wall has shown to convert to hydrate when entering the relevant P, T domain. Furthermore, the tests will be able to reveal fundamental knowledge of a generic kind.
In general, the results from this work suggest that hydrates will stick less to surfaces with low surface energy and when the surrounding oil has a high concentration of acids.
Experiments with model systems can also be useful for explaining results obtained in experiments with crude oils, as shown in the next section.

### *Real oil systems*

Experiments from a crude oil system are presented in Table 5. The oil tested here gives a contact angle larger than any of the model oil experiments performed on glass (see Table 3). The angle and the resulting adhesion energy are compared with the model oil system containing 5000 ppm of acids, which was presented in Tables 3 and 4. The contact angle is larger for the crude oil system compared to the model oil system. However, due to different interfacial tensions of the systems, the adhesion energies for the systems are quite similar. Hence, the surface is rendered more oil-wet from contact with the crude oil, but the brine does not adhere any stronger to it.

Table 5: Contact angles and adhesion energies of brine on glass in crude oil, and in a model oil with 5000 ppm acids.

| Oil phase | Contact angle $\theta$ (degrees) | Interfacial tension mJ/m$^2$ | Adhesion energy mJ/m$^2$ |
|---|---|---|---|
| Crude oil | $86 \pm 6$ | 33 | $35 \pm 3$ |
| Model oil | $40 \pm 3$ | 20 | $36 \pm 1$ |

The amount of extracted acids of the B4c oil is determined to be 11.8 mg/g oil [25]. This is a concentration of 11 800 ppm of acids. At this point no experiments has been performed on higher concentrations than 5000 ppm. However, the contact angle will probably remain unchanged after a certain concentration from the surface sites being filled, as shown for the metal surfaces.

## CONCLUSIONS

The wettabilty of pipeline surface material has been measured after exposure to oil. Petroleum acids are found to render all the surfaces more oil wet.
The effect of acids on the adhesion in a brine/oil/solid system has also been tested. The results show that:

- The adhesion energy between brine and solid surface in oil depends on the solid surface material. The adhesion energies can be correlated to the initial solid surface energies of the surfaces.
- Acids affect the adhesion in the sense that an increase in acid concentration leads to a reduction in adhesion and more oil-wet conditions.
- Preliminary experiments with epoxy coated surfaces indicate that surface roughness can have an effect on the adhesion in brine/solid/oil systems.
- It is indicated that hydrates will stick less to the pipeline surfaces when acids are present in the oil.

## ACKNOWLEDGMENTS

StatoilHydro and Chevron ETC are acknowledged for funding and permission to publish data. The Norwegian Research Council, the Petromaks program, is thanked for funding.
The HYADES project group consists of experienced research personnel from both university, research institution and industry, that actively participates in planning of activities and discussion of results. The in-kind contributions from both university and industry partners are of essential value for the quality of the project, and are thus highly appreciated. The project group consists of the following persons:

- SINTEF Petroleum Research: Roar Larsen, David Arla, Sylvi Høiland, and Jon Harald Kaspersen.
- University of Bergen: Tanja Barth, Alex Hoffmann, Pawel Kosinski, Anna E. Borgund, Guro Aspenes (PhD student), Boris Balakin (PhD

student), Ziya Kilinc (MSc student), and Håkon Pedersen (MSc student).

- Chevron ETC (Houston): Ramesh Kini, Lee Rhyne, and Hari Subramani.
- StatoilHydro: Per Fotland and Kjell M. Askvik.

Arta AS is acknowledged for providing the metal samples.

## REFERENCES

[1] Høiland Standal S. *Wettability of solid surfaces induced by adsorption of polar organic components in crude oil.* Dr.Scient. (PhD equivalent) thesis, Department of Chemistry, University of Bergen, Norway, 1999.

[2] Høiland S, Askvik KM, Fotland P, Alagic E, Barth T, Fadnes F. *Wettability of freon hydrates in crude oil/brine emulsions.* J. Coll. Int. Sci. 2005;287:217-225.

[3] Taylor CJ, Dieker LE, Miller KT, Koh CA, Sloan Jr. ED. *Micromechanical adhesion force measurements between tetrahydrofuran hydrate particles.* J. Coll. Int. Sci. 2007;306:255-261.

[4] Høiland S, Borgund AE, Barth T, Fotland P, Askvik KM. *Wettability of freon hydrates in crude oil/brine emulsions: The effects of chemical additives. In: Proceedings of the 5th International Conference on Gas Hydrate.* 2005;4:1151-1161.

[5] York JD, Firoozabadi A. *Comparing effectiveness of rhamnolipid biosurfactant with quaternary ammonium salt surfactant for hydrate anti-agglomeration.* J. Phys. Chem. B 2008;112:845-851.

[6] Young T. *Miscellaneous Works, Vol. 1.* London: Murray, 1855. p. 418.

[7] Marcus P. *Surface science approach of corrosion phenomena.* Electrochimica Acta 1998;43:109-118.

[8] Hashimoto K, Asami K, Kawashima A, Habazaki H, Akiyama E. *The role of corrosion-resistant alloying elements in passivity.* Corros. Sci. 2007;49:42-52.

[9] Pardo A, Merino MC, Coy AE, Viejo F, Arrabal R, Matykina E. *Effect of Mo and Mn additions on the corrosion behavior of AISI 304 and 316 stainless steel in $H_2SO_4$.* Corros. Sci. 2007;in press.

[10] Robin R, Miserque F, Spagnol V. *Correlation between composition of passive layer and corrosion behavior of high Si-containing austenitic stainless steels in nitric acid.* J. Nuc. Mater. 2008;in press.

[11] Askvik KM, Høiland S, Fotland P, Barth T, Grønn T, Fadnes FH. *Calculation of wetting angles in crude oil/water/quartz systems.* J. Coll. Int. Sci. 2005;287:657-663.

[12] Adamson AW. *Physical chemistry of surfaces.* fifth ed. John Wiley & Sons, New York, 1990.

[13] Gunde R, Kumar A, Lehnart-Batar S, Mäder R, Windhab EJ. *Measurement of the surface and interfacial tension from maximum volume of a pendant drop.* J. Coll. Int. Sci. 2001;244:113-122.

[14] Spelt JK, Li D. *The equation of state approach to interfacial tensions.* In: Neumann AW, Spelt JK, editors. Applied Surface thermodynamics. New York: Marcel Dekker, 1996. p. 239-292.

[15] Kwok DY, Neumann AW. *Contact angle measurements and contact angle interpretation.* Adv. Coll. Int. Sci. 1999;81:167-249.

[16] Padday JF. *Apparatus for measuring the spreading coefficient of a liquid on a solid surface.* J. Sci. Instruments 1959;36:256-257.

[17] Tyson WR, Miller WA. *Surface free energies of solid metals: Estimation from liquid surface tension measurents.* Surf. Sci. 1977; 62:267-276.

[18] Israelachvili J. *Intermolecular and surface forces. With applications to colloid and biological systems.* Academic Press, 1985. p. 149-151.

[19] Podgornik B, Zajec B, Strnad S, Stana-Kleinschek K. *Influence of surface energy on the interactions between hard coatings and lubricants.* Wear 2007;262:1199-1204.

[20] Chen PJ, Wallace RM, Henck SA. *Thermal properties of perfluorinated n-alkanoic acids self-assembled on native aluminum oxide surfaces.* J. Vac. Sci. Technol. A 1998;16:700-706.

[21] van der Brand J, Blajiev O, Beentjes PCJ, Terryn H, de Wit JHW. *Interaction of anhydride and carboxylic acid compounds with aluminum oxide surfaces studied using infrared reflection absorption spectroscopy.* Langmuir 2004;20:6308-6317.

[22] Allara DL, Nuzzo RG. *Spontaneously organized molecular assemblies. 2. Quantitative infrared spectroscopic determination of equiibrium structures of solution-adsorbed n-alkanoic acids on an oxidized aluminum surface.* Langmuir 1985;1:52-66.

[23] Chen SH, Frank CW. *Infrared and fluorescence spectroscopic studies of self-assembled n-alkanoic acid monolayers.* Langmuir 1989;5:978-987.

[24] M*ü*ller B. *Corrosion inhibition of different metal pigment in aqueous alkaline media.* Corros. Sci. 2001;43:1155-1164.

[25] Borgund AE, Erstad K, Barth T. *Fractionation of crude oil acids by HPLC and characterization of their properties and effects on gas hydrate surfaces.* Energy & Fuels 2007;21:2816-2826.